# Optical detection of electron paramagnetic resonance for intrinsic defects produced in ZnO by 2.5-MeV electron irradiation *in situ* at 4.2 K

L. S. Vlasenko* and G. D. Watkins
*Department of Physics, Lehigh University, 16 Memorial Drive East, Bethlehem, Pennsylvania 18015-3182, USA*
(Received 14 February 2005; published 6 July 2005)

Intrinsic defects produced in ZnO by 2.5-MeV electron irradiation *in situ* at 4.2 K are studied by optical detection of electron paramagnetic resonance (ODEPR). Observed in the photoluminescence (PL) are ODEPR signals, which are identified with the oxygen vacancy, $V_O^+$, interstitial zinc, $Zn_i^+$, and zinc-vacancy–zinc-interstitial Frenkel pairs. The Frenkel pairs are primarily observed in their $S=1$ exchange-coupled state, supplying strong evidence that interstitial zinc is a shallow effective mass double donor in ZnO. Annealing stages at ~65–119 K and ~145–170 K are observed for the defects associated with the zinc sublattice and are identified with the migration of interstitial zinc. Although interstitial oxygen is not observed in the ODEPR, a higher-temperature annealing stage observed in the PL at ~160–230 K is tentatively identified with the onset of its migration. The oxygen vacancy is stable to ~400 °C. The relationship between the spin-dependent processes producing the ODEPR signals and the PL of the material remains unclear.

DOI: 10.1103/PhysRevB.72.035203 PACS number(s): 61.72.Ji, 61.82.Fk, 76.70.Hb, 78.55.Et

## I. INTRODUCTION

There is currently growing interest in zinc oxide (ZnO) as a wide band-gap semiconductor for possible electronic and optical applications. Readily grown as large single crystals, with a bandgap of ~3.4 eV, it potentially offers many complementary and/or competitive advantages in these applications to the similar band-gap material GaN, to which it provides, in addition, a close lattice match.[1]

Important to its successful device application is the understanding of its intrinsic defects, i.e., vacancies and interstitials, because they provide the various diffusion mechanisms involved in processing and device degradation, as well as often controlling, directly or indirectly, background doping, compensation, minority carrier lifetime, and luminescence efficiency. The only direct and unambiguous method for introducing vacancies and interstitials for experimental studies is by high-energy electron irradiation, where single host atoms can be displaced from their lattice sites by recoil from an electron-nucleus Rutherford scattering event. In order to assure that the properties of the simple primary defects are being monitored, the irradiation should be performed at a sufficiently low temperature to freeze them in before migration can occur.

The most successful experimental technique for identifying and studying the defects has often proven to be electron paramagnetic resonance (EPR), detected either directly or optically [optical dectection of EPR (ODEPR)]. In the case of ZnO, early EPR studies in the 1970s have already identified vacancies produced by electron irradiation at room temperature on each of the two sublattices—$V_{Zn}^-$ and $V_{Zn}^0$ on the Zn sublattice,[2–4] and $V_O^+$ on the O sublattice.[5,6] In those studies, they were found to be stable at room temperature. More recent studies have suggested that the oxygen vacancy is stable to ~400 °C.[7]

Information concerning the host atom interstitials in ZnO, however, has only recently begun to emerge. This comes from a recent study of our group,[8] where the effect of 4.2 K irradiation by 2.5-MeV electrons was monitored by ultraviolet (UV) excited photoluminescence (PL) and optical detection of electron paramagnetic resonance in the PL. In this preliminary study, it was found that several below-room-temperature annealing stages in the PL occurred, and three ODEPR signals were observed to emerge and disappear approximately accompanying the stages. None of the ODEPR signals were identified but, because the vacancies on the two sublattices, had already been established to be stable at room temperature, it could be concluded that one or both of the interstitials on the two sublattices must be mobile at these cryogenic temperatures to account for the annealing stages.

In the present paper we extend the 4.2 K *in situ* electron irradiation studies to further probe the processes and defects involved. In studying more heavily irradiated samples, and including visible wavelength excitations as well, we observe several new ODEPR signals, and an additional lower-temperature annealing stage at ~65 K. Several of the new ODEPR signals are identified as arising from zinc-vacancy–zinc-interstitial close Frenkel pairs. In addition, ODEPR signals from the oxygen vacancy and interstitial zinc are identified, present also directly after the electron irradiation.

## II. EXPERIMENTAL

For the study, ZnO samples were cut from nominally undoped 0.5 mm thick single {0001} crystal wafers obtained from two different sources: (i) Eagle Picher, labeled EP, grown by seeded chemical vapor transport, and (ii) University Wafer Inc., labeled UW, for which the original growth method was unspecified.

The experimental setup used to obtain the data described in this paper is identical to that of earlier ODEPR work on ZnSe, which should be referred to for further details.[9] Briefly, the experiments were performed at 20 GHz in an EPR spectrometer capable of irradiation *in situ* at 4.2 K with 2.5-MeV electrons from a Van de Graaff accelerator. Subsequent PL and ODEPR experiments were accomplished by

 

inserting into the $TE_{011}$ microwave cavity a fused quartz capillary tube, which served as a light pipe to extract the photoluminescence (PL) and within which was threaded an optical fiber that allowed for optical excitation of the sample (located a few millimeters below the light pipe). To monitor the PL and the ODEPR signals, the luminescence was detected with either a silicon (EG&G 250UV) or cooled germanium (North Coast EO-817S) diode detector, and excitation ($\leqslant$20 mW) was supplied by the various UV and visible lines available from an argon-ion laser. The PL spectra were determined using a Jarrell Ash 0.25 m monochromator and were subsequently corrected for monochromator and detector responses. For the measurements, the samples were immersed in pumped liquid helium ($\sim$1.7 K). For the ODEPR experiments, microwave power from a 300 mW Gunn diode was on-off modulated at various frequencies from 10 to 1000 Hz, and synchronous changes in the luminescence were detected via lock-in detection. In one case, the (0001) Zn-surface of the sample was indium-soldered onto a brass post, cut at 45° in order to provide equal O-surface area for the horizontal electron irradiation and subsequent vertical photoexcitation. (The magnetic field could be rotated in the horizontal plane and therefore only directions between $\mathbf{B} \perp c$ axis and 45° to the $c$ axis were accessible.) For the other experiments, the sample was indium soldered onto a post such that its $c$ axis was in the horizontal plane allowing full angular studies from $\mathbf{B} \| \mathbf{c}$ to $\mathbf{B} \perp \mathbf{c}$. In this case, the reduced sample area for vertical optical excitation and PL detection was still found to be adequate for the study.

## III. PREVIOUS RESULTS

In our earlier preliminary 4.2 K *in situ* 2.5-MeV electron irradiation studies,[8] the primary result was the introduction of a broad double-humped PL, centered at $\sim$750 and 900 nm, with partial suppression of the PL bands initially present in the material. No new ODEPR signals were observed prior to annealing. The first annealing stage appeared to occur over the region $\sim$110–140 K, with the disappearance of the double-humped band and the emergence of two weak negative ODEPR signals, labeled L1 and L2. A second annealing stage occurred in the range $\sim$160–230 K, where a broad PL band centered at $\sim$680 nm emerged accompanied by the disappearance of L1 and L2 and the emergence of a stronger new negative signal L3 accompanied by an equally intense negative signal of the shallow effective mass (EM) donor. In a third annealing stage at $\sim$300 K, the 680 nm PL band disappeared along with the L3 and EM ODEPR signals, and the PL and ODEPR returned approximately to their original preirradiation values. None of the PLODEPR signals were identified.

In this first study, the electron irradiation dose was modest ($\sim 1.4 \times 10^{16}$ e/cm$^2$) and only excitation with the UV lines of the argon laser (351.1 or 363.8 nm) were used. In a more recent study employing a heavier 2.5-MeV electron irradiation dose ($3\text{-}9 \times 10^{17}$ e/cm$^2$) at room temperature, and extension to include visible wavelength excitations, it was discovered that a significant concentration of the negative L3 signal actually remains present at room temperature along

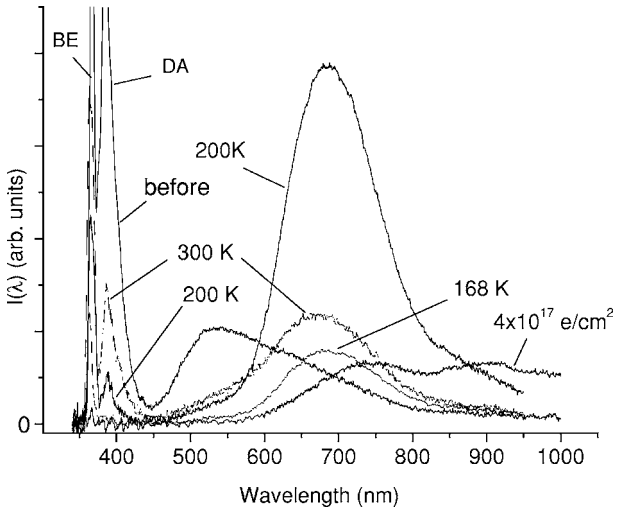


FIG. 1. PL spectra of the EP sample under 364 nm excitation at 1.7 K. Shown are the spectra before and after 2.5-MeV electron irradiation *in situ* at 4.2 K, and after selected 30 min annealing stages.

with the 680 nm band, both being stable to $\sim$400 °C.[7] In that study it was shown also that it is seen as a positive signal in a band at 600 nm with a weak tail extending well into the near infrared. In addition, more precise measurements of the L3 $g$ values revealed it to arise from the positively charged oxygen vacancy $V_O^+$, by comparison to the earlier extensive EPR studies of it.[5,6] In the low-temperature *in situ* irradiation studies, it was being observed indirectly, only as a spin-dependent electron transfer from the shallow donor to it, which is *competing* with the 680 nm band, emerging and disappearing with it. Taken together the two studies suggest that in the anneal at room temperature, a fraction of the 680 nm band disappears, but some remains stable to $\sim$400 °C. The oxygen vacancy is stable to $\sim$400 °C and is observed in electron transfer from distant shallow donor to it both in competition with the 680 nm band and in direct contribution to a band at 600 nm.

Another study, upon which we will rely significantly in our interpretation of the results in this paper, is that of EPR, PL, and ODEPR for low-temperature *in situ* MeV electron-irradiated ZnSe.[9–14] In that remarkable case, isolated zinc interstitials and vacancies were observed directly, as well as $\sim$25 well-resolved close Frenkel pairs of different separations in the lattice. By monitoring their behavior versus annealing it was possible to unambiguously unravel much of the complex annealing processes involved. The results for that II-VI material will serve as a helpful guide in the interpretation of the results here for ZnO, which manifest themselves, however, in a interestingly different way for the ODEPR signals.

## IV. RESULTS

In Fig. 1, the PL under 364 nm UV excitation for the EP sample is shown before, after $4 \times 10^{17}$ e/cm$^2$ irradiation with 2.5-MeV electrons *in situ* at 4.2 K, and after a few representative 30 min isochronal anneals. The results are similar to

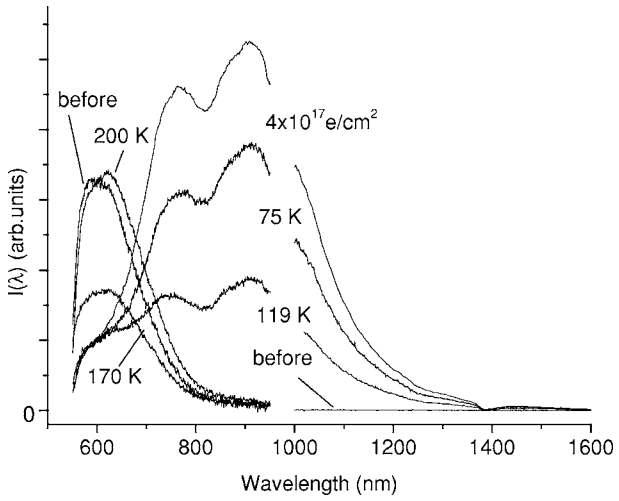


FIG. 2. PL spectra of the UW sample under 457.9 nm excitation at 1.7 K. Shown are the spectra before and after 2.5-MeV electron irradiation *in situ* at 4.2 K, and after selected 30 min annealing stages. (The dip at ~1400 nm is an artifact resulting from absorption in the quartz light pipe used to extract the PL from the cryostat.)

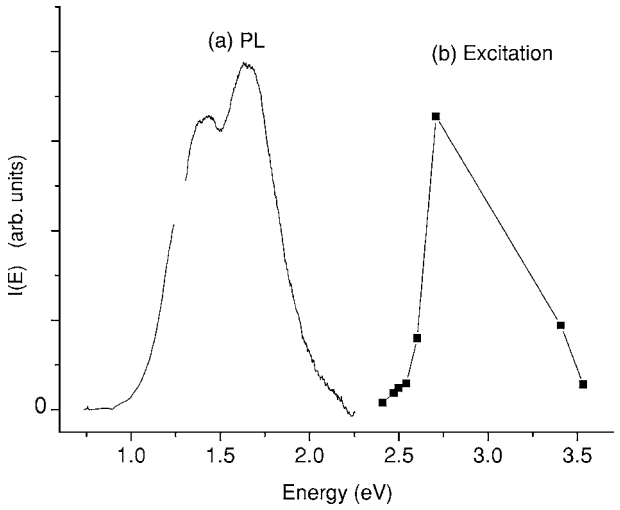


FIG. 3. Energy dependence of (a) the irradiation-produced IR band and (b) its excitation spectrum as determined by the intensity of the band vs excitation at each of the visible and UV argon laser lines.

those reported in the earlier studies by our group after $1.4 \times 10^{16}$ e/cm$^2$,[8] the principal effect of the irradiation being the generation of a broad double-humped band (at ~750 and ~900 nm) in the near infrared (IR), and suppression of the neutral donor bound exciton (BE), shallow donor-acceptor (DA), and broad ~540 nm preirradiation bands. The same three major annealing stages are observed: ~110–150 K with the disappearance of the double-humped IR band, ~180–230 K with the emergence of the 680 nm band, and ~300 K, with partial return to the preirradiation PL state. The major difference in this more heavily irradiated case is the initial stronger suppression of the preirradiation bands, and, in the final recovery stage, the persistence of a substantial fraction of the 680 nm band and only partial recovery of the original bands.

The PL under UV excitation for the UW sample is similar, with production of the double-humped IR band of comparable intensity and suppression of the preirradiation bands, followed by the same major annealing stages. The major difference is that the for the UW sample, the preirradiation PL shows no near-band-edge neutral donor-bound exciton or shallow DA pair luminescence, instead displaying only a very strong broad and different visible luminescence band at ~600 nm. The irradiation-produced suppression of this band is not as great, and in the higher-temperature annealing stages, its recovery dominates the PL so that the emergence and partial recovery of the 680 nm band in the ~180–230 K and ~300 K stages, although still observable, is less apparent.

In Fig. 2, we show the PL results for the UW sample under excitation with the 457.9 nm visible line of the argon laser. With this excitation wavelength, we find the radiation-produced IR band much stronger and better suited for the ODEPR studies. The reason for this is illustrated in Fig. 3, where the intensity of the irradiation-produced IR band is shown versus the excitation energy for constant intensity of the various argon-ion laser lines. The same behavior is observed in the EP sample. The dependence suggests either an excitation band centered ~3.0 eV or, alternatively, an above-band-gap band that tails into the gap supplying the most effective excitation at the highest energy available argon-ion laser line (457.9 nm), which is sufficiently less than the gap to allow bulk penetration of the sample. The ODEPR studies that we describe in what follows have therefore been primarily performed under the visible excitation lines of the laser.

In Fig. 4, the ODEPR observed in the UW sample under visible excitation is shown 4(a) before and 4(b) after $4 \times 10^{17}$ e/cm$^2$ irradiation with 2.5-MeV electrons *in situ* at 4.2 K, and (c) and (d) after selected anneals. Before, the strong ODEPR spectrum of spin-dependent DA pair recombination between distant shallow single donors (which we label EM throughout the present paper) and deep substitutional Li acceptors[15,16] dominates,

$$\mathrm{EM}^0 + \mathrm{Li}_{\mathrm{Zn}}^0 \rightarrow \mathrm{EM}^+ + \mathrm{Li}_{\mathrm{Zn}}^-, \tag{1}$$

and its spectral dependence follows accurately the broad 600 nm band associated with it. This spectrum is not present in the EP material and supplies a strong hint that the UW material was prepared by the hydrothermal growth process, which often uses LiOH as a solvent in the process.[17] (Present also is a sharp isotropic negative line of unknown origin, labeled *Y*, present undiminished throughout the irradiation and annealing sequence. It is most strong under low-frequency modulation, or dc conditions, reflecting a slow recombination process with the EM donor.) After the irradiation, the $\mathrm{Li}_{Zn}^0$ ODEPR is suppressed, which in Fig. 4(b) has been further suppressed, but still visible, by insertion of a filter that passes only $\lambda > 665$ nm. Four new signals have emerged, which we have labeled $\mathrm{V}_{\mathrm{Zn}}^{\prime -}$, $\mathrm{V}_0^+$, $\mathrm{V}_{\mathrm{Zn}}^{\prime\prime -}$/EM, and $\mathrm{Zn}_i^+$ in the figure. The justification for these labels will be apparent in what follows. The spectral dependence of each of these signals, determined by the application of selective fil-

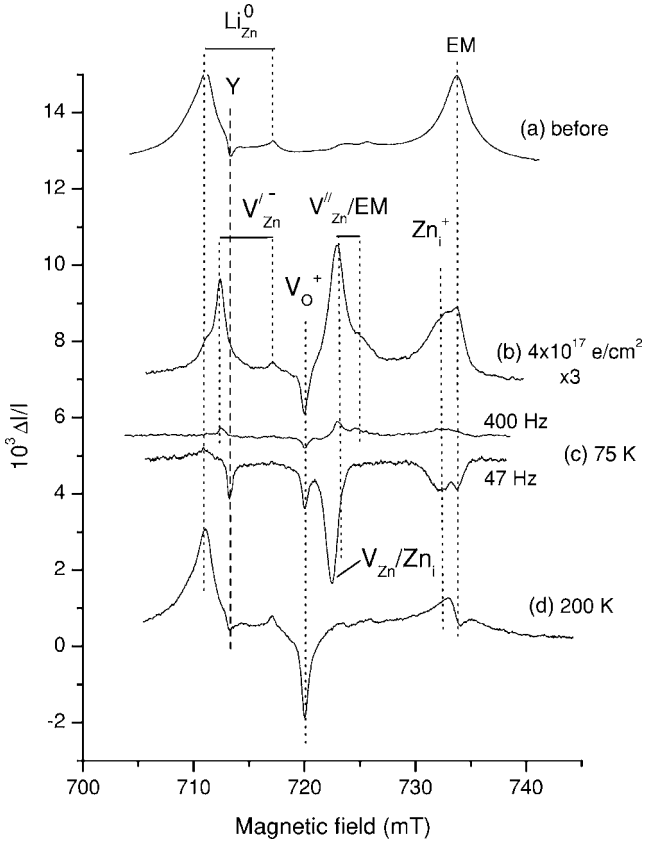


FIG. 4. ODEPR spectra observed in the UW sample, **B**∥c-axis, before and after 2.5-MeV electron irradiation at 4.2 K, and after selected 30 min. anneals. The detection parameters (excitation wavelength, spectral region for detection, and modulation frequency) differed somewhat for the various measurenents, being optimized in each case for best signal to noise. After the 75 K anneal, (c), different spectra appear at the two modulation frequencies indicated.

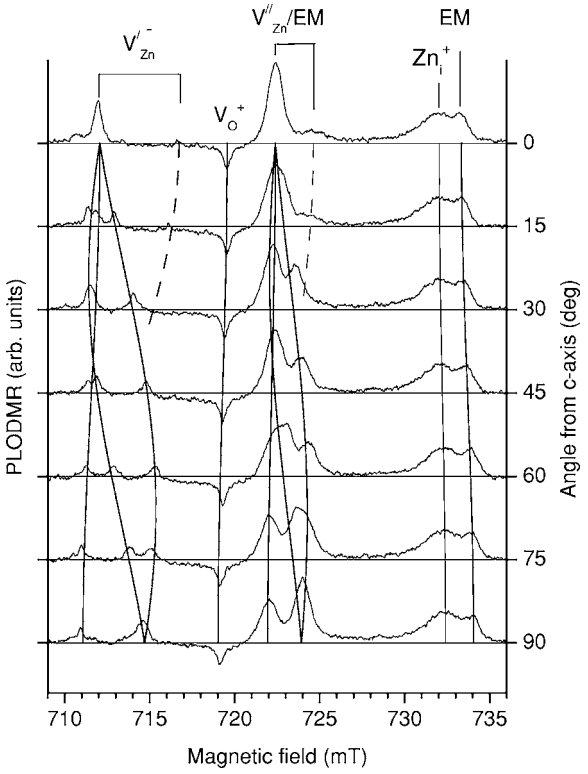


FIG. 5. Angular dependence of the ODEPR spectra with **B** in the (1100) plane for the UW sample immediately after the 4.2 K electron irradiation.

ters before the detector, appears to accurately reflect the broad double-humped PL band produced by the irradiation. These ODEPR signals are also observed in the EP sample, but their strengths were consistently weaker. In what follows, therefore, we will concentrate primarily on the ODEPR results in the UW sample.

In Fig. 5, we show the angular dependences of the spectra with **B** in the (1100) plane, and in Table I we list the $g$ values determined for the spectra. We note first from its $g$ values that $V_0^+$ is actually present immediately after the irradiation. This differs from the earlier low-dose 4.2 K irradiation experiments where the spectrum (labeled L3 in that study) was not observed to appear until the 160–230 K annealing stage.[8] The present observation is as expected, of course, for an intrinsic defect produced by the electron irradiation and further confirms the $V_0^+$ identification[7] with the L3 spectrum.

Next, we note that the $g$ values determined for $V'^-_{Zn}$ are very close to those previously determined by EPR for the isolated zinc vacancy, which are also included in the table. This is evident in Fig. 6, where the individual $g$ values calculated from the experimentally measured magnetic-field positions for the nonaxial $V'^-_{Zn}$ centers in Fig. 6 are compared directly to that predicted from the EPR determined parameters for isolated $V^-_{Zn}$. (In ZnO,[2–4] as well as in the other zinc chalcogenides ZnS,[26] and ZnSe,[10] a trigonal Jahn-Teller distortion occurs for $V^-_{Zn}$, the trapped hole localizing primarily on one of the four nearest neighbors. In wurtzite ZnO, the axial and nonaxial centers are inequivalent, the nonaxial ones being energetically preferred and significantly stronger.) The agreement is very good, perhaps within the experimental error of our measurements. On the other hand, recognizing that the slight departure could be real, we have tentatively labeled it $V'^-_{Zn}$, the prime being added to include the possibility that the zinc vacancy is weakly perturbed by the presence of its nearby $Zn_i$ Frenkel partner. Seeing it in ODEPR as a simple $S=1/2$ center along with the $S=1/2$ EM donor signal suggests that the spin-dependent process being observed is electron transfer

$$V'^-_{Zn} + EM^0 \rightarrow V'^{2-}_{Zn} + EM^+, \quad (2)$$

where the donor is sufficiently distant from $V'^-_{Zn}$ so that the exchange interaction between them is weak.

Finally, consider the spectrum labeled $V''_{Zn}$/EM. Its lines are broader and less well resolved than those for $V'^-_{Zn}$, but the form of its angular dependence in Fig. 5 is clearly similar to that of $V'^-_{Zn}$, with the exception only that its angular anisotropy is approximately one-half of that for $V'^-_{Zn}$ and it is centered approximately halfway between it and the EM signal. This supplies a strong hint as to its origin: For an $S=1$ state made up from two exchange-coupled $S=1/2$ defects, the $g$ values should be given, to a good first approximation, simply by the average between the $g$ values for the two. In Fig. 7(a),

TABLE I. Spin-Hamiltonian parameters for the defects. For the nonaxial centers, the $z$ and $x$ axes are in a {1120} reflection symmetry plane, with $\theta$, the angle between the $z$ and $c$ axes.

| | | Axial | | Nonaxial | | | |
|---|---|---|---|---|---|---|---|
| Center | $S$ | $g_\parallel$ | $g_\perp$ | $g_{xx}$ | $g_{yy}$ | $g_{zz}$ | $\theta$(deg) |
| EM[a] | 1/2 | 1.9570 | 1.9551 | | | | |
| $Li_{Zn}^{0}$ [b] | 1/2 | 2.0028(3) | 2.0253(3) | 2.0223(3) | 2.0254(3) | 2.0040(3) | 112.6(5) |
| $V_O^{+}$ [c] | 1/2 | 1.9945(2) | 1.9960(2) | | | | |
| $V_O^{+}$(L3) | 1/2 | 1.9946(2) | 1.9960(2) | | | | |
| $V_{Zn}^{-}$ [d] | 1/2 | 2.0024 | 2.0193 | 2.0173(2) | 2.0183(2) | 2.0028(2) | 110.75(25) |
| $V_{Zn}'^{-}$ | 1/2 | 2.0024(5) | | 2.0175(2) | 2.0188(2) | 2.0033(2) | 110.75[e] |
| $V_{Zn}''^{-}$ | 1/2 | | | 2.0183(5) | 2.0207(5) | 2.0041(5) | 110.75[e] |
| $V_{Zn}''$/EM | 1 | | | 1.9976(3) | 1.9879(3) | 1.9797(3) | 110.75[e] |
| $V_{Zn}/Zn_i$ | 1 | | | 1.9888(4) | 1.9893(5) | 1.9815(4) | 110.75[e] |
| $Zn_i^{+}$ | 1/2 | 1.9605(3) | 1.9595(3) | | | | |

[a]Reference 18. These values were used for magnetic field calibration.
[b]Reference 16.
[c]Reference 6.
[d]Reference 3.
[e]Not adjusted. Taken as equal to that in Ref. 3

we test this by comparing the nonaxial $g$ values for $V_{Zn}''$/EM determined from the measured magnetic-field positions in Fig. 5, with that predicted by the average of the values determined for EM and $V_{Zn}'^{-}$ given in Table I. The agreement is not perfect, but is close, clearly indicating that we have correctly identified the origin of the spectrum as arising from an $S=1$ exchange-coupled state made up from a separated shallow donor and a zinc-vacancy-related center. The agreement can be made perfect by solving for the $g$ values of the zinc-vacancy-related defect that, combined with the EM $g$ values, would be required to match the $V_{Zn}''$/EM values shown by the solid lines in Fig. 7(a). These values, now labeled $V_{Zn}''^{-}$, are given in Table I, and the corresponding angular dependence for them is shown also in Fig. 6. Again the small departures between these $g$ values and those for isolated $V_{Zn}^{-}$ are well within that expected for the perturbation of a close interstitial zinc, as evidenced by the direct evidence for close Frenkel pairs in ZnSe.[10,11] (It would also be possible to get a good match in Fig. 7(a) using the $V_{Zn}'^{-}$ $g$ values if the partner donor $g$ value was taken to be isotropic at $g=1.9570$, but we see no convincing evidence for the existence of such a donor.) We conclude, therefore, that the $V''_{Zn}$/EM spectrum arises from a spin-dependent process similar to Eq. (2),

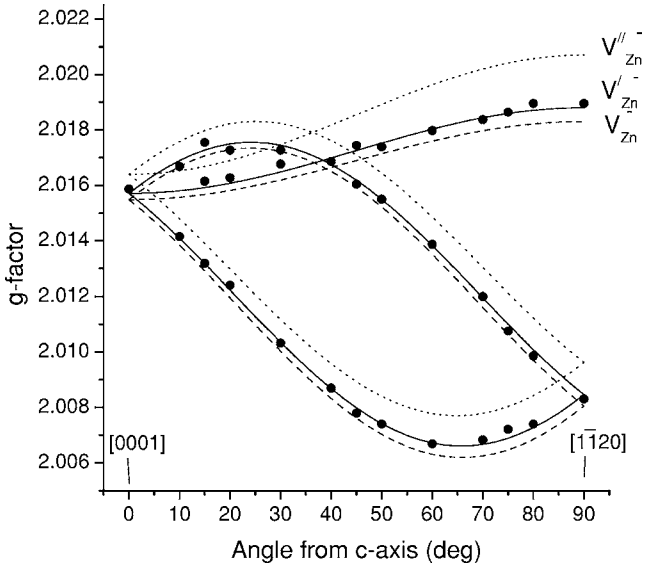


FIG. 6. Angular dependence of the $g$ factors determined for the nonaxial $V_{Zn}'^{-}$ centers (solid lines and experimental points) and $V''_{Zn}$ (dotted lines), compared to the corresponding values for isolated $V_{Zn}^{-3}$ (dashed lines).

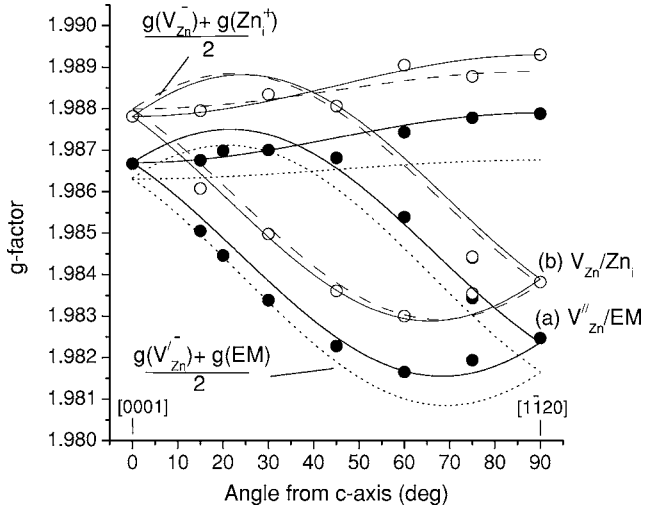


FIG. 7. Angular dependence of the $g$ values for (a) the nonaxial $V_{Zn}''$/EM spectrum (solid lines and closed circle experimental points), compared to the prediction (dotted lines) for an $S=1$ coupled $V_{Zn}'$ and EM pair; and (b) the $V_{Zn}/Zn_i$ spectrum (solid lines and open experimental points) compared to the prediction (dashed lines) for an $S=1$ coupled $V_{Zn}$ and $Zn_i$ pair.

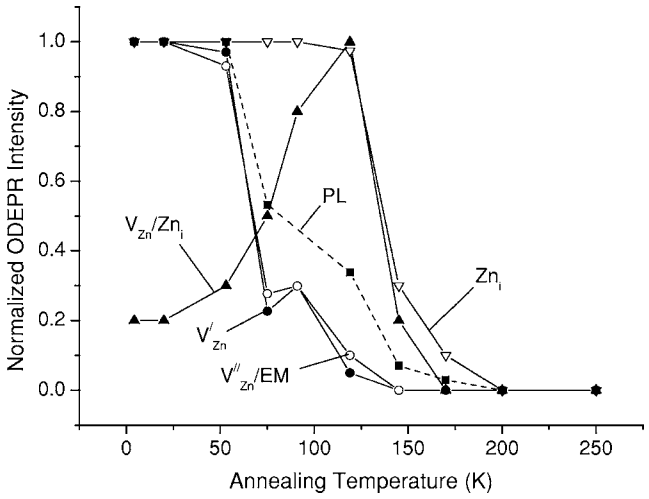


FIG. 8. Normalized intensity of the irradiation-produced ODEPR signals ($\Delta I/I$ for each) and that of the double-humped PL vs 30 min isochronal annealing temperature.

$$V''^{-}_{Zn} + EM^{0} \rightarrow V''^{2-}_{Zn} + EM^{+}, \quad (3)$$

where, in this case, the exchange interaction is large enough with a closer EM donor to produce the combined $S=1$ spectrum.

After a 30 min anneal at 75 K, Fig. 4(c), both the $V'^{-}_{Zn}$ and $V''_{Zn}$/EM have decreased strongly. Upon further 30 min anneals at 119 and 145 K, both spectra have completely vanished. This is summarized in Fig. 8. (Plotted in the figure are the fractional changes in the PL, $\Delta I/I$, for the ODEPR signals. The actual decrease in the $V'^{-}_{Zn}$ and $V''_{Zn}$/EM signals is greater at each stage, being given by the product of $\Delta I/I$ and the PL intensity, which is also shown in the figure.) At the same time, already after the 75 K anneal in Fig. 4(c), a new spectrum becomes dominant, similar to $V''_{Zn}$/EM but shifted slightly to lower magnetic fields, which is negative and observed only at lower-modulation frequencies, as shown. A careful check of the spectrum before anneal at low-modulation frequencies reveals that it was apparently also present there, but weaker.

A possible origin for this spectrum is apparent in Fig. 7(b), where the angular dependence of its dominant lines are also plotted. (There appear to be additional weaker lines present which cannot be easily resolved.) As shown in the figure, the $g$ values of these lines can be accurately simulated by the average of the EPR determined $g$ values for isolated $V^{-}_{Zn}$ and that of the broad signal displaced to slightly lower magnetic field from the EM signal. This strongly suggests that the spin-dependent recombination process now finally being observed is that expected between $S=1$ exchange-coupled Frenkel pairs of the Zn sublattice,

$$V^{-}_{Zn} + Zn^{+}_{i} \rightarrow V^{2-}_{Zn} + Zn^{2+}_{i}, \quad (4)$$

which serves, in turn, to finally suggest the identification of the broad signal near the EM signal as arising from interstitial $Zn^{+}_{i}$, as labeled in Figs. 4 and 5, and Table I. We label this $S=1$ Frenkel pair spectrum $V_{Zn}/Zn_i$ and include its $g$ values also in Table I. (The errors indicated in Table I for $V_{Zn}/Zn_i$ and $V''_{Zn}$/EM reflect the estimated absolute accuracy of these broader, less resolved $S=1$ spectra. The two spectra were taken essentially at the same time, only at different modulation frequencies, so their relative accuracy is substantially better.) In Fig. 2, the broad double-humped PL line is still present after the 119 K anneal. However, the spectral dependence of the negative $V_{Zn}/Zn_i$ spectrum no longer mimics it, but rather is stronger for wavelengths $\lambda > 1000$ nm. Also, its greatest intensity is produced with the longer wavelength excitation, 514.5 nm. The fact that the signals are strongest at low-modulation frequencies reveals a slow limiting process in the ODEPR detection, which could be either the Frenkel pair recombination itself or the unrelated luminescence process with which it is competing.

Upon further 30 min isochronal anneals, the $V_{Zn}/Zn_i$ and $Zn^{+}_{i}$ spectra are both significantly reduced at 150 K, with $V_{Zn}/Zn_i$ disappearing completely at 170 K, and $Zn^{+}_{i}$ at 200 K. These results are also summarized in Fig. 8. The ODEPR results at 200 K are shown in Fig. 4(d), where the Li DA signals have essentially returned to their original values, the only difference from the before irradiation result being the remaining negative $V^{+}_{O}$ and EM signals. No significant change is observed upon subsequent room-temperature anneal.

The same electron irradiation-produced ODEPR spectra ($V^{+}_{O}, V'^{-}_{Zn}, V''_{Zn}$/EM, $V_{Zn}/Zn_i$, and $Zn^{+}_{i}$) are also observed in the EP sample. However, there are differences in detail: (i) In the EP sample, the ODEPR signals are uniformly weaker ($\sim \times 3$). (ii) As in the UW sample, $V^{+}_{O}$ is observed directly after the 4.2 K *in situ* irradiation, but in the EP sample it is a positive signal, not negative. It remains positive until the 160–200 K anneal where it becomes negative, along with a corresponding negative EM signal, resulting from its competition with the strong emerging 680 nm band (see Fig. 1). After the 300 K anneal, it is still negative in the remaining 680 nm band, but can be seen to be positive in both shorter (a band at $\sim$600 nm) and longer wavelength PL regions. This behavior is consistent with the earlier lower dose 4.2 K *in situ* electron-irradiation studies for an EP sample,[8] where the negative $V^{+}_{O}$(L3) signal emerged and disappeared with the 680 nm band but was too weak to be observed before the emergence of the 680 nm band, or after its disappearance. The PL spectral-dependence behavior after the 300 K anneal is identical to that after a similar high-dose electron irradiation at room temperature of an EP sample, which has been extensively studied.[7] (iii) After a $4\times10^{17}$ e/cm$^2$ *in situ* electron irradiation of the EP sample, all of the spectra observed in the UW sample are present except for $V'^{-}_{Zn}$. Upon increasing the dose to $6\times10^{17}$ e/cm$^2$, $V'^{-}_{Zn}$ emerges. The EP annealing behavior is similar to the UW results, Fig. 8, with $V'^{-}_{Zn}$ and $V''_{Zn}$/EM disappearing in the 65–100 K region, and $Zn^{+}_{i}$ disappearing in the 150–200 K region. However, the $V_{Zn}/Zn_i$ signal, observed weakly before the first 65–85 K anneal, is not observed after that anneal.

Finally, the negative L1 and L2 spectra, previously observed in the earlier lower-dose 4.2 K irradiation studies,[8] were also observed here to emerge weakly in both the EP and UW samples upon anneal in the 110–140 K stage and to disappear in the 160–230 K stage. They were observed only under UV excitation, however, suggesting possibly that they

are near-surface related. They will not be discussed further in the present paper.

## V. DISCUSSION

Both the EP and UW samples reveal essentially the same behavior. In the PL, Figs. 1 and 2, the electron irradiation suppresses the UV and visible bands initially present and produces a broad double-humped band centered at ~750 and 900 nm. This band disappears upon anneal in two stages over the region ~65–150 K, and a band at 680 nm emerges at ~180–230 K. The 680 nm band anneals partially at ~300 K, with partial return of the sample to its preirradiation state. The main difference between the PL for the two is the dominance of the strong deep Li DA band at ~600 nm in the UW sample, which significantly masks the emergence and partial recovery of the 680 nm band as the Li DA band recovers upon anneal. The same irradiation-produced ODEPR signals are also observed in both samples, and they display essentially the same annealing behavior. However, the signals are stronger in the UW sample, and the $V_{Zn}/Zn_i$ signal, not observed after the 65–85 K anneal in the EP sample, remains observable in the UW sample as a negative signal up to ~150 K. Also, in the UW sample, the $V_O^+$ signal is negative, whereas in the EP sample it is positive before the emergence of the strong 680 nm band with which it competes and becomes negative. We conclude that the differences between the two samples reflect primarily the presence of the substitutional Li acceptor in the UW material. In the case of the negative $V_O^+$ and $V_{Zn}/Zn_i$ signals, the presence of the Li acceptor supplies its strong deep DA pair luminescence, never completely quenched (Fig. 2), with which they compete. An additional factor, particularly in accounting for the stronger signals in the UW sample, may also be the compensation supplied by the Li acceptor, allowing more efficient optical excitation of the defect charge states involved in the spin-dependent ODEPR processes. Here, therefore, we have presented primarily the results for the UW sample, where more of the processes could be followed, and with a better signal-to-noise ratio. We conclude that they are fully representative of the fundamental intrinsic defect processes in ZnO, made more easily observable only indirectly by the Li acceptor doping.

### A. ODEPR

The identifications that we have made for the various irradiation-produced ODEPR signals follow from the following arguments: In the first place, high-energy electron irradiation can only displace atoms. Therefore, all of the ODEPR signals produced by the 4.2 K *in situ* irradiation must originate from intrinsic defects—primarily lattice vacancies and/or host atom interstitials, either isolated or in close Frenkel pair configurations. From their $g$ values, the identification of the oxygen vacancy $V_O^+$ and the Zn vacancy-related signal $V'^-_{Zn}$ follow immediately. Also, from their $g$ values, the identification of both the $V''_{Zn}$/EM and $V_{Zn}/Zn_i$ ODEPR spectra as $S=1$ centers made up from Zn vacancy-related defects exchanged-coupled to EM-like donors also follows directly. In the case of $V''_{Zn}$/EM, the best fit requires the donor to have $g$ values very close to those of the EM single donor, leading, therefore, to the identification of the Zn vacancy-related defect as $V''_{Zn}$, a Zn vacancy slightly perturbed by the nearby presence of its Frenkel partner, presumably $Zn_i^{2+}$. The angular dependence of the $V_{Zn}/Zn_i$ $g$ values is very similar to that for $V''_{Zn}$/EM, but shifted to higher values by approximately one-half the difference between the single donor EM values and those for the irradiation-produced broad signal to slightly lower magnetic fields, which we have labeled $Zn_i^+$ in Figs. 4 and 5. This strongly suggests the donor in that case to be that giving rise to the broad line near EM and, working back from its $g$ values, leads to a close $g$ value match to that of isolated $V^-_{Zn}$. Since we anticipate spin-dependent recombination between the Frenkel pairs on the Zn sublattice, as has been observed in ZnSe,[9,12,13] this leads directly to the identification of the broad ODEPR line as that of $Zn_i^+$. Consistent with this, the broad ODEPR line must be associated with an intrinsic defect and, of the remaining two, $Zn_i$ or $O_i$, only the Zn interstitial is expected to be a donor. Further confirmation comes from theoretical predictions that conclude that interstitial zinc should introduce no deep levels in the gap[19,20] and is, therefore, only an effective-mass-like double donor. Since the paramagnetic $Zn_i^+$ state is its singly ionized state, its electrical level position should be ~4× deeper than that of a neutral single donor (i.e., $\sim E_C - 0.2$ eV), supplying an explanation for its small positive $g$ shift from the single-donor EM values.

What we are seeing is remarkably similar to what has been observed in ZnSe. In that well-studied case, a first annealing stage was also observed to occur at ~65–80 K, at which point a very close Frenkel pair on the Zn sublattice, observed by ODEPR as recombination between a distant shallow donor and the pair, disappeared.[9,12] (From EPR studies, it was determined that annihilation of the pair had not actually occurred. Instead, the interstitial in that case actually migrated around to a more stable position directly behind a Se near neighbor to the vacancy.[10,11] However, this configuration was not detected in the ODEPR,[9,12] so that, as here in ZnO for the $V''_{Zn}$/EM signals that we interpret also as arising from recombination of close pairs with a distant EM donor, only the disappearance is observed by ODEPR.) In addition in ZnSe, recombination between the partners of many distinct $Zn_i$-$V_{Zn}$ pairs were detected in the ODEPR, the closest annealing first, the more distant persisting to ~260 K, where the zinc interstitial, also observed by ODEPR, also disappeared. In ZnO, we observe the disappearance of the pairs $(V_{Zn}/Zn_i)$ and $Zn_i$ at a somewhat lower temperature, ~150–200 K. This suggest a somewhat lower barrier for $Zn_i$ migration in ZnO, but otherwise essentially the same processes appear to be being observed in both materials.

If we are correct in our interpretation of the results in ZnO, there are clearly important differences in how the spin-dependent processes manifest themselves in the ODEPR, which we now consider. In ZnSe, recombination between pairs of different separations were well resolved, four very close pairs being exchange-coupled $S=1$ systems, distin-

guishable by different fine structure terms, and 20 less strongly coupled pairs where the ODEPR of the individual members of each pair were resolved with different splittings, revealing directly the exchange interaction in each case.[9] Here in ZnO, none of this highly detailed structure is being observed. Instead, with the exception of $V'^{-}_{Zn}$ and $Zn_i^+$, all other spectra are observed as $S=1$ systems, with no resolvable evidence of fine structure. This is true for the $V''_{Zn}$/EM system, which we interpret as involving recombination between a close pair and a distant EM single donor, as well as for the $V_{Zn}/Zn_i$ system, which we interpret as involving direct recombination between the two members of Frenkel pairs on the Zn sublattice, of differing separations.

The reason for these differences can be explained in terms of a different character for the $Zn_i^+$ donor state in the two cases. In ZnSe, the $(+/++)$ donor-level position has been estimated experimentally to be deep at $\sim E_C - 0.9$ eV, the $Zn_i^+$ wave function being highly localized with a Bohr radius of only $\sim 1.78$ Å.[9] This deep character was also predicted by theory.[22] In ZnO, as already pointed out above, theory predicts no deep level for $Zn_i^+$, its wave function, therefore, being effective-mass-like at $\sim E_C - 0.2$ eV and much more spread out, with a Bohr radius of $\sim 7$ Å. This means that in ZnO, the exchange between $V_{Zn}^-$ and $Zn_i^+$ drops off much more slowly versus separation. To this must be added the requirement that $J \gg (\Delta g \mu_B B)^2$ for a simple $S=1$ spectrum to emerge, where $J$ is the exchange interaction, and $\Delta g$ is the difference between the $g$ values for $V_{Zn}^-$ and $Zn_i^+$.[23] With a maximum $g$ value difference in ZnSe of 0.1186,[9] compared to the value in ZnO of 0.0588 (Table I), this further means that the exchange interaction in ZnO needs be only 25% of that in ZnSe in order to make transitions within the $S=1$ state dominate. Finally, the fine structure splittings in the $S=1$ state derive primarily from magnetic dipole-dipole interactions between the $S=1/2$ Frenkel partners. In the case of ZnSe, with both being highly localized, the dipole-dipole interaction can reflect primarily that between spins located at each of the two lattice sites even for the relatively close pairs, and indeed has been used as a means to estimate the separation of the pairs.[9] However, the dipole-dipole interaction between a highly localized $V_{Zn}^-$ wave function and a diffuse overlapping one for a nearby $Zn_i^+$ will be strongly reduced because it is the angular anisotropy of the interaction averaged over the two wave functions that provides the fine structure term. All of this supplies, in turn, strong further confirmation that, as predicted from theory, $Zn_i$ produces no deep levels in ZnO[19,20] and, therefore, is simply an effective-mass double donor. (Because the theoretical estimates involved a very large extrapolation from a calculated band gap of only 0.6–0.9 eV to the true value of 3.4 eV, their predictions could well have been suspect. Our results, however, appear to supply the necessary confirmation.)

There is an additional possible difference with regard to the properties of $Zn_i$ in the two materials, which we now consider. In ZnSe, $Zn_i$ has been shown to migrate in the lattice under optical excitation even at 1.5 K.[14] This has been confirmed directly where optical excitation causes $Zn_i^+$ interchange between its more stable site surrounded by four Se neighbors and its site surrounded by four Zn neighbors, such a move corresponding to one-half of a single diffusional jump. It also manifests itself as interconversion between the various resolved close Frenkel pairs observed under prolonged excitation at that temperature. No evidence of such optically induced motion has been observed thus far in our present studies in ZnO, although it may be more difficult to detect since the individual pairs are not resolved. In ZnSe, the driving force for the phenomenon was suggested to be electron captured into an excited $p$-like state, which Jahn-Teller distorts supplying a kick to the central $Zn_i$ atom in the diffusion direction.[14] Optically induced migration was found to be away from its partner vacancy, indicating capture either into a neutral state, as for EL2 in GaAs, or possibly into a negative charge state that goes deep, as for DX in GaAlAs.[24] Both are more likely when $Zn_i$ tends to introduce deep states as in ZnSe, possibly explaining the difference here also. We caution, however, that a more extended study would be necessary to completely exclude the possibility that it is also occurring in ZnO.

Next, consider the broad $S=1/2$ ODEPR line that we have identified with $Zn_i^+$. It is present along with the $V_{Zn}/Zn$ $S=1$ signal up to the 150–200 K annealing stage. However, the broad $S=1/2$ signal must arise from those $Zn_i^+$ interstitials that are not recombining with their partner vacancy as $S=1$ centers. In addition, because no accompanying $S=1/2$ $V_{Zn}^-$ signals are present, the spin-dependent processes in which they are involved must involve defects other than their Frenkel partners. One possibility is electron transfer from distant single shallow EM donors to them,

$$Zn_i^+ + EM^0 \rightarrow Zn_i^0 + EM^+. \quad (5)$$

Non-spin-dependent recombination could then follow with the nearby $V_{Zn}^-$ Frenkel partner, the electron being transferred from nonparamagnetic $Zn_i^0$. This could also supply an explanation for the $Zn_i^+$ ODEPR signal breadth as arising from a distribution of exchange interactions between it and the distant EM donor.

There remain two possibilities for the identification of the $S=1/2$ $V'^{-}_{Zn}$ ODEPR signal. Its $g$ values are very close to those of isolated $V_{Zn}^-$, see Table I and Fig. 6. It could therefore result from spin-dependent electron transfer from a distant EM donor to a zinc vacancy that is sufficiently distant from its Frenkel partner to behave as isolated. Or it could be an additional close Frenkel pair, apparently distinct from $V''^{-}_{Zn}$, to which electron transfer from a distant donor is occurring. The fact that it disappears in the first annealing stage along with $V''_{Zn}$/EM argues for its identification as a close pair. However, since its appearance itself is apparently very fragile (in the EP sample, observed at a dose of $6 \times 10^{17}$ e/cm$^2$, but not at $4 \times 10^{17}$ e/cm$^2$), we cannot fully rule out the first possibility, the disappearance resulting indirectly instead from pseudo-Fermi-level change, for example, associated with the $V''^{-}_{Zn}$ anneal.

### B. PL

Consider now the PL and its relationship to the ODEPR signals. Before any anneal, there is the single irradiation-produced broad double-humped PL band (at $\sim$750 and 900

nm), within which positive ODEPR signals of $V'^{-}_{Zn}$, $V''_{Zn}$/EM, and $Zn_i^+$ are observed. This suggests that it is related in some way to the intrinsic defects produced by displacements on the Zn sublattice. When $V'^{-}_{Zn}$ and $V''_{Zn}$/EM disappear upon anneal at 75–119 K, approximately one-third of the broad PL band remains (see Fig. 8), with no observable change in shape. In fact, the shape of the PL seems to be unchanged also versus production during the irradiation, the optical excitation energy, and different ZnO samples, suggesting that it is the property of a single optical transition. This, in turn, suggests connecting it, therefore, with transitions from shallow EM donor to close pairs such as $V''_{Zn}$/EM, and possibly $V'^{-}_{Zn}$, and with some additional such pairs, not seen by ODEPR, remaining after they disappear. The PL band finally disappears in the region 145–170 K, roughly similar to the anneal of $V_{Zn}/Zn_i$, which arises from spin-dependent recombination between $V^-_{Zn}$ and its Frenkel partner $Zn_i^+$. However, these ODEPR signals are negative and originate from longer wavelengths than the band.

In ZnSe, the PL for the corresponding transition from shallow EM to closest Frenkel pair, $V^-_{Zn}+Zn_i^{2+}$ ("V$^{\prime\prime}$"), is at a shorter wavelength, ~600 nm (2.07 eV),[12] which is 0.42 eV greater than the value for the ZnO transition at ~750 nm (1.65 eV). Adding to that the band-gap difference of 0.65 eV between that for ZnO (3.45 eV) and ZnSe (2.80 eV) would appear to require that the $(2-/-)$ level position for $V_{Zn}$ be ≈1.07 eV higher in the gap in ZnO than in ZnSe, if it is the same transition, and if the JT energy is the same in ZnO and ZnSe. Is that reasonable? First consider theory: We note that Kohan *et al.*[19] predicted the $(2-/-)$ level for $V_{Zn}$ in ZnO to be at $E_V+0.9$ eV, which is indeed 0.9 eV higher in the gap than predictions of similar calculations for ZnSe at $E_V-0.03$ eV.[22] On the other hand, Zhang *et al.*[20] predicted the level to be at the valence band edge, essentially the same as for the ZnSe result. Recently, Van de Walle has suggested it to be ⩽0.5 eV above the valence band edge after further calculations.[21] Let us, therefore, take, for example, $E_V+0.3$ eV. The experimentally determined $(2-/-)$ level in ZnSe is actually at $E_V+0.66$ eV, the discrepancy with the theoretical prediction of $E_V-0.03$ eV in that case being partially accounted for by the experimentally determined ~0.35 eV JT distortion,[25] which raises the level in the gap and was not included in the calculations either in ZnSe or ZnO. The remainder of the discrepancy, ~0.34 eV, presumably reflects a modest error in the theoretical result. Assuming the same JT energy in ZnO, and otherwise the same amount of additional error in the theoretical estimate, the 0.3 eV difference would appear to apply also to the real level positions, which, by itself, is clearly much less than the 1.07 eV required to explain the double-humped PL band as resulting from the distant shallow EM donor to close pair transition. However, the JT energy for $V^-_{Zn}$ in ZnO, which is small polaron in character on one of the four neighboring second-row oxygen-atom neighbors, might be significantly larger than that for the fourth-row Se-atom neighbor. This has the effect of raising the level further in the gap by the difference in the JT energy and, in turn, reducing the apparent 1.07 eV level position difference by twice that amount because of the additional Stokes shift reduction in the transition energy. Evidence of this already exists for the case of the vacancy in ZnS, where the experimentally estimated JT energy was determined to be ~0.52 eV,[26] compared to the 0.35 eV value for ZnSe.[25] Indeed, if we were to interpret the excitation spectral dependence for the double-humped PL in Fig. 3 as the reverse of the PL process, a total Stokes shift of ≈1.5 eV is indicated, corresponding to a total relaxation energy of ≈0.75 eV, of which the $V_{Zn}$ JT energy would presumably provide the major part. This is clearly not out of line with the Se to S trend, so it is a possibility. With the implied increase in the JT energy over that for ZnSe of ~0.4 eV, the transition energy is reduced by twice that, ~0.8 eV, which, with the 0.3 eV theoretically estimated level position difference, adds up to ~1.1 eV, as required.

Consider a different method by which to make an estimate for the energy expected for the distant shallow EM donor to close Frenkel pair transition in ZnO, which does not rely on theoretical estimates of the zinc vacancy level position: In ZnSe, the PL band for recombination from a distant shallow EM donor to the isolated $V^-_{Zn}$ is at 720 nm (1.72 eV),[27] to $V^-_{Zn}$ with a compensating $Cl^+$ donor as nearest neighbor ("A-center") is at 620 nm (2.0 eV),[27] and to the closest Frenkel pair $V^-_{Zn}+Zn_i^{2+}$ ("V$^{\prime\prime}$") is at 600 nm (2.07 eV).[12] Each of these defects is basically $V^-_{Zn}$, but which, in the case of the latter two, is singly compensated by a donor at the nearest-neighbor site or doubly compensated by a double donor at twice the distance away. The effect of this is to lower the level of the defect in the band gap by ~0.28 and ~0.35 eV, respectively. In ZnO, we have the result in Fig. 1 that the PL associated with distant shallow donor to $Li^0$ acceptor recombination is at ~600 nm (2.07 eV). Here again the $Li^0$ acceptor is, for all practical purposes, simply $V^-_{Zn}$ with a singly compensating closed shell $Li^+$ donor ion inside. If we assume that, as in ZnSe, the close $Li^+$ single donor lowers the level position roughly the same as its nearest double-donor Frenkel pair partner $Zn_i^{2+}$, the transition for the close Frenkel pair is then predicted to be also at ~600 nm (2.07 eV), which is ~0.4 eV higher than the observed transition at ~750 nm (1.65 eV). This discrepancy is not great and could possibly result either from underestimating the level lowering by the $Li^+$ ion in the center of the vacancy or overestimating the vacancy JT energy when it has the $Li^+$ ion in its center or both.

From these considerations, we are forced to conclude that it is *possible*, but by no means certain, that the double-humped near-IR PL band in ZnO arises directly from shallow EM to close $V^-_{Zn}+Zn_i^{2+}$ Frenkel pair recombination, as seen in the $V''_{Zn}$/EM and possibly the $V'^{-}_{Zn}$ ODEPR signals.

There remain two additional possibilities for the origin of the double-humped PL band that should be considered: (i) The PL could instead result primarily from the transition of distant shallow EM donors to $V^-_{Zn}$'s sufficiently distant from their Frenkel partners to appear isolated, a possibility for $V'^{-}_{Zn}$. With the isolated vacancy $(2-/-)$ level ~0.35 eV higher in the gap than that for the close pair, each of our level-position estimates above would have less difficulty in accounting for the PL. This may be more difficult to rationalize, however, in terms of an overall logical interpretation of the results. (ii) The PL need not be a spin-dependent process, and, in that case, it could still involve intrinsic defects

associated with the Zn-sublattice. Coupled with the spin-dependent electron transfer processes being observed in our ODEPR signals, the double-humped PL could result from subsequent hole capture as part of the total PL pumping cycle, involving, therefore, a nonparamagnetic charge state of the $V_{Zn}$-related defect involved. In that case, however, the $(2-/-)$ level of $V_{Zn}$ would have to be much higher in the gap than the theoretical calculations are indicating to account for the 750 nm (1.65 eV) hole-capture transition energy. [The transition energy of the broad Stokes-shifted transition is equal to the true level position above the valence band minus the JT energy. But since the calculations do not include the JT relaxations, the calculated values should approximate the optical transition energy. Therefore, if the transition is to the isolated vacancy, the calculated value for its $(2-/-)$ level should be giving $\sim E_V+1.65$ eV. If it is to the close pair the calculated vacancy level should be $\sim 0.35$ eV higher at $\sim E_V+2.0$ eV.] If one believes the current calculated values for the unrelaxed vacancy,[19–21] they would appear to rule out hole capture either by an isolated $V_{Zn}^{2-}$ or a close Frenkel pair.

Another important question is why the double humps? As stated earlier, the shape of the PL appears to be constant (versus production during the irradiation, the various stages of anneal, the optical excitation energy, and the different ZnO samples), suggesting that it is the property of a single optical transition. Probably the simplest explanation is that it reflects complex energy surfaces associated with the vacancy Jahn-Teller relaxation as the core of the defect goes from its JT-relaxed $V_{Zn}^{-}$ configuration to its unrelaxed $V_{Zn}^{2-}$ state, or vice versa. This is certainly possible, particularly when, for ZnO, it has been found that $V_{Zn}^{-}$ undergoes a trigonal distortion,[2–4] and $V_{Zn}^{0}$ undergoes an entirely different dihedral distortion,[3] consistent with complex energy surfaces associated with its JT distortions.

PL associated with the direct recombination between Zn-sublattice Frenkel partners is apparently not being observed, the corresponding $V_{Zn}/Zn_i$ transitions being detected only as negative ODEPR signals. We can also predict where the PL for these transitions might be expected to be by comparison again with their positions in ZnSe, where they are observed from $\sim$800 nm (1.55 eV) for very close pairs to $\sim$1100 nm (1.13 eV) for the more distant ones.[9] To these, we must take into account the 0.7 eV difference between the $Zn_i$ second donor-level positions for the two semiconductors ($\sim E_C-0.2$ eV in ZnO, $\sim E_C-0.9$ eV in ZnSe) plus the 0.65 eV band-gap difference, which places the $(+/2+)$ level for $Zn_i$ 1.35 eV higher above the valence band edge in ZnO compared to ZnSe. Even, therefore, if the $(2-/-)$ $V_{Zn}$ level is 1.07 eV higher in ZnO, or if this difference comes primarily from the greater JT energy as suggested above, this still leaves the predicted energy difference between the level positions for the zinc vacancy and zinc interstitial to be $1.35-1.07=0.28$ eV greater in ZnO. How much higher in energy the pair transitions should be is a little trickier to predict for pairs of different separations because of the difficulty in estimating the Coulomb contributions in the case of the shallower $Zn_i^{+}$ in ZnO, but in the limit of the very distant pairs it should begin to approach the full 0.28 eV difference, the longer wavelength 1100 nm value in ZnSe approaching $\sim$880 nm in ZnO. All of the closer pairs should be at shorter wavelengths. This argues that the PL should therefore be observed if the transitions are radiative.

The failure to find a region in the PL spectrum where the $V_{Zn}/Zn_i$ ODEPR signals are positive argues, therefore, that these transitions are not radiative. This, in turn, provides an additional argument for significantly larger JT lattice relaxation associated with the transitions in ZnO than in ZnSe, so that the energy can be more effectively converted instead into phonon production. Unfortunately, theory may not be able to help us here, the current LDA techniques not having been able to duplicate, thus far, the experimentally established large symmetry lowering distortions for the zinc vacancy in either ZnSe (Ref. 22) or ZnO.[19]

The other prominent PL band that is clearly related to defects produced by the irradiation is the 680 nm band, which emerges in the range $\sim$160–230 K and partially disappears at 300 K. Directly correlated with it is the emergence and partial disappearance of the negative $V_O^{+}$ and accompanying EM signals. But, being negative, they are only competing with the PL band, ruling out a direct involvement in its production. No positive ODEPR signals are seen in it. Since $Zn_i^{+}$ disappears at a somewhat lower temperature and both the zinc and oxygen vacancies are stable at and above room temperature, this suggests that the emergence of the 680 nm band may be related to the onset of interstitial oxygen migration.

## VI. SUMMARY

After irradiation by 2.5 MeV electrons *in situ* at 4.2 K, ODEPR observed in the PL has revealed the oxygen vacancy, $V_O^{+}$, interstitial zinc, $Zn_i^{+}$, and a few dominant zinc vacancy-related defects, $V_{Zn}^{-}$, $V_{Zn}^{\prime-}$, and $V_{Zn}^{\prime\prime-}$. $V_{Zn}^{\prime-}$ and $V_{Zn}^{\prime\prime-}$ are observed in a spin-dependent electron transfer from a distant EM donor and disappear in an annealing stage covering the temperature range 65–119 K. $V_{Zn}^{\prime\prime-}$ has been identified as a close $V_{Zn}^{-}+Zn_i^{2+}$ Frenkel pair, but whether $V_{Zn}^{\prime-}$ is also such a pair or simply $V_{Zn}^{-}$ sufficiently removed from its Frenkel pair partner to behave as isolated could not be established. Persisting in the ODEPR to $\sim$150–170 K is the zinc vacancy $V_{Zn}^{-}$, which is observed in a spin-dependent electron transfer from its nearby $Zn_i^{+}$ Frenkel-pair partner. The ODEPR of $Zn_i^{+}$ disappears completely by 200 K, but the $V_O^{+}$ signal remains until a $\sim$400 °C anneal. Because the zinc vacancy has been established by previous EPR studies to be stable at room temperature,[2–4] the various annealing stages for the defects produced from the Zn sublattice must reflect the migration of interstitial zinc.

The results are remarkably similar to those previously established for defects of the zinc sublattice in ZnSe, where a close Frenkel pair also disappeared in a first annealing stage at 65–80 K, whereas spin-dependent transfer between other Frenkel pairs could continue to be followed as they annealed at higher temperatures, closer pairs first, with the most distant persisting to $\sim$260 K, where the interstitial zinc also disappeared.[9–13] Here also the zinc vacancy was known to be stable at room temperature,[28] establishing that the annealing stages resulted from migration of the interstitial.

The character of the ODEPR signals associated with the Zn sublattice in ZnO depart strongly, however, and in an interesting way from that observed in ZnSe, where each of the Frenkel pairs of different separation could be resolved and independently studied. In ZnO, with the exception of the $S=1/2$ $V_{Zn}^{\prime -}$ and $Zn_i^+$ signals, all of the Frenkel pairs give exchange-coupled $S=1$ signals, distinguishable only by their $g$ values as to whether they involve a distant EM donor or the nearby $Zn_i^+$ Frenkel-pair partner as the electron source, and with no resolvable distinction versus the pair separation. The reason for this difference can be explained if interstitial zinc introduces no deep levels in ZnO and is therefore an effective mass double donor with a much more extensive electron wave function in its singly ionized $Zn_i^+$ state. This has been predicted from theoretical studies of two different groups,[19,20] and our results supply, experimental confirmation of that prediction.

The PL also differs significantly from the ZnSe results, where resolvably different bands could be unambiguously identified with each of the different ODEPR-resolved Frenkel-pair processes. In our studies here in ZnO, that has not been the case. In fact, it is not clear whether PL is actually being observed for any of the spin-dependent processes being observed in the ODEPR. They do not appear to be being observed for the direct transitions between Zn sublattice Frenkel pairs, and it may also be the case for distant-donor to close-pair transitions if the double-humped PL actually arises from subsequent non-spin-dependent hole capture in the pumping cycle. On the other hand, we have shown that the possibility that the double-humped PL band results directly from distant EM donor to close Frenkel pair, or possibly to the isolated zinc vacancy, cannot be ruled out. Clearly a critical issue in unraveling these questions is the magnitude of the JT relaxation for the zinc vacancy in ZnO, which plays a vital role both in the estimate for the origin of the double-humped band, and, separately, in helping to explain the nonradiative character for the transitions. Because the currently popular local density calculations are apparently not capable of handling the symmetry-lowering JT distortions of the zinc vacancy, this question may ultimately have to be addressed by experiment, as was the case only after extensive experiments for ZnSe and ZnS. At the same time, this should serve as a strong challenge to theorists to properly address why LDA often seems to fail in handling local symmetry-lowering relaxations, and in particular, to find a way to solve the problem.

Finally, the emergence of a PL band at 680 nm in an annealing stage at 160–230 K appears sufficiently separated from the annealing processes associated with the zinc sublattice defects to suggest that it may be associated with the onset of migration for the oxygen interstitial.

## ACKNOWLEDGMENTS

We gratefully acknowledge helpful discussions with Y. V. Gorelkinskii, W. B. Fowler, M. S. Stavola, and C. G. Van de Walle. We thank also G. Cantwell for supplying the Eagle Picher material. The research was supported by the National Science Foundation, Grant No. DMR-00-93784.

*Present address: A. F. Ioffe Physico-Technical Institute, Russian Academy of Sciences, 194021, St. Petersburg, Russia.

[1] See the recent review by D. C. Look, Mater. Sci. Eng., B **80**, 383 (2001).

[2] A. L. Taylor, G. Filipovich and G. K. Lindeberg, Solid State Commun. **8**, 1359 (1970).

[3] D. Galland and A. Hervé, Phys. Lett. **A33**, 1 (1970).

[4] D. Galland and A. Hervé, Solid State Commun. **14**, 953 (1974).

[5] J. M. Smith and V. H. Vehse, Phys. Lett. **A31**, 147 (1970).

[6] C. Gonzales, D. Galland and A. Hervé, Phys. Status Solidi B **72**, 309 (1975).

[7] L. S. Vlasenko and G. D. Watkins, Phys. Rev. B **71**, 125210 (2005).

[8] Yu. V. Gorelkinskii and G. D. Watkins, Phys. Rev. B **69**, 115212 (2004)

[9] F. C. Rong, W. A. Barry, J. F. Donegan, and G. D. Watkins, Phys. Rev. B **54**, 7779 (1996)

[10] G. D. Watkins, Phys. Rev. Lett. **33**, 223 (1974).

[11] G. D. Watkins, in *Lattice Defects in Semiconductors, 1974*, edited by F. A. Huntley, IOP Conf. Proc. No. 23 (Inst. of Physics, London, 1975), p. 338.

[12] F. Rong and G. D. Watkins, Phys. Rev. Lett. **56**, 2310 (1986).

[13] W. A. Barry and G. D. Watkins, Phys. Rev. B **54**, 7789 (1996).

[14] K. H. Chow and G. D. Watkins, Phys. Rev. B **60**, 8628 (1999).

[15] R. T. Cox, D. Block, A. Hervé, R. Picard, C. Santier, and R. Helbig, Solid State Commun. **25**, 77 (1978).

[16] O. F. Schirmer, J. Phys. Chem. Solids **29**, 1407 (1968).

[17] T. Sekiguchi, S. Miyashita, K. Obara, T. Shishido, and N. Sakagumi, J. Cryst. Growth **214/215**, 72 (2000).

[18] W. E. Carlos, E. R. Glaser, and D. C. Look, Physica B **308-310**, 976 (2001).

[19] A. F. Kohan, G. Ceder, D. Morgan, and Chris G. Van de Walle, Phys. Rev. B **61**, 15019 (2000). In this paper, deep levels are predicted for interstitial zinc. However, Van de Walle (private communication) (Ref. 21) informs us that in that result, the band-gap correction was not properly handled, and that no deep levels in the gap should have been predicted for interstitial zinc.

[20] S. B. Zhang, S.-H. Wei, and Alex Zunger, Phys. Rev. B **63**, 075205 (2001).

[21] C. G. Van de Walle (private communication).

[22] D. B. Laks, C. G. Van de Walle, G. F. Neumark, P. E. Blöchl, and S. T. Pantelides, Phys. Rev. B **45**, 10 965 (1992).

[23] This follows directly from simple diagonalization of the $2\times 2$ submatrix for the spin Hamiltonian of two $S=1/2$ defects coupled by $JS_1\cdot S_2$.

[24] G. D. Watkins, Semicond. Sci. Technol. **6**, B111 (1991). In this paper, a description of the EL2 and DX phenomena is given as

capture into excited *p* states which go deep as they Jahn-Teller distort.

[25] G. D. Watkins, in *Defect Control in Semiconductors*, edited by K. Sumino (North-Holland, Amsterdam, 1990), p. 933.

[26] K. H. Lee, K. P. O'Donnell, and G. D. Watkins, Solid State Commun. **41**, 881 (1982)

[27] K. H. Lee, Le Si Dang, and G. D. Watkins, Solid State Commun. **35**, 527 (1980).

[28] G. D. Watkins, in *Radiation Effects in Semiconductors*, edited by J. W. Corbett and G. D. Watkins (Gordon and Breach, London, 1971), p. 301.